Available online at www.sciencedirect.com
ScienceDirect
International Journal of Heat and Mass Transfer 50 (2007) 4461–4467
International Journal of HEAT and MASS TRANSFER
www.elsevier.com/locate/ijhmt

Theoretical prediction and experimental verification of temperature distribution in FGM cylindrical plates subjected to thermal shock

T. Sadowski [a,*], M. Boniecki [b], Z. Librant [b], K. Nakonieczny [c]

[a] Faculty of Civil and Sanitary Engineering, Department of Solid Mechanics, Lublin University of Technology, Nadbystrzycka 40 str., 20-618 Lublin, Poland
[b] Institute of Electronic Materials Technology, Wólczyńska 133 str., 01-919 Warszawa, Poland
[c] Faculty of Mechanical Engineering, Lublin University of Technology, Nadbystrzycka 36, 20-618 Lublin, Poland

Available online 28 June 2007

Abstract

This paper focuses on the problem of temperature field and evaluation of the heat transfer coefficient in FGM cylindrical plates subjected to thermal shock. The cylindrical plates are made of five ceramic layers: purely Al_2O_3 layer and composite layers made of Al_2O_3 matrix and 5, 10, 15, 20 wt% content of ZrO_2. The problem is solved in two stages. First, the heat transfer coefficient on the thermal shock surface is estimated by fitting the experimental data with calculated temperatures for a monolithic plate made of alumina. Then, the obtained heat transfer coefficient is used for prediction of the temperature field in the FGM plate subjected to the same boundary conditions. After comparison with the experimental data, the heat conduction characteristics of the alumina/zirconium composite can be estimated.

Keywords: FGM ceramic material; Thermal shock; Heat transfer; Temperature distribution

1. Introduction

The modern FGM composite materials have a complex internal structure due to the fact that they consist of several different phases. Mechanical and thermal properties of composites depend on the constituent features as well as their spatial distribution. There are two typical kinds of FGM materials: (1) with continuous changes of the material properties, (2) with discrete variation of the composite features. An example of the first type FGM is a so called gradient zone created by technological process between coating and substrate of many structural parts subjected to temperature loadings, e.g. [1,2]. The discrete variation of properties is exhibited by multilayered composites – very popular for many engineering applications. An example of this composite type can be ceramic matrix composites (CMC) structure made of purely Al_2O_3 layer and additional composite layers with additives of different materials: metal or ceramic.

Many structural elements applied in mechanical or aircraft engineering e.g. are subjected to temperature gradient. A typical example is structural ceramics, which is used as a thin layer in high-temperature engines because of its excellent heat resistance. Other applications are thermal barrier coatings for turbines, shuttle buses, etc. However, ceramics are brittle or semi-brittle not only at room temperature but also at elevated temperatures, and they are sensitive to the thermal stress caused by step temperature gradients, i.e. thermal shock. Thus, a precise evaluation of the ceramics properties at thermal shock is essential for its reliable application in high-temperature structures.

One of the methods, which help to better understand the properties of FGM, relays on subjecting a specimen to thermal shock, which is realised frequently in a jet impingement system. This can be realised in laboratory experiments or by

* Corresponding author. Tel.: +48 81 538 13 86; fax: +48 81 525 69 48.
E-mail address: t.sadowski@pollub.pl (T. Sadowski).

0017-9310/$ - see front matter © 2007 Elsevier Ltd. All rights reserved.
doi:10.1016/j.ijheatmasstransfer.2007.05.002

means of numerical simulations. The latter method is more efficient, but has to be based on some model that predicts the heat transfer coefficient distribution on the specimen surface. The early studies in this field have been concentrated mainly on experimental predictions of heat transfer from impinging jets, which is reviewed by Jambunathan et al. [3]. Further inclusions into the field are made, for example, by Peper et al. [4], Yan and Saniei [5], Siba et al. [6] and Baydar et al. [7]. However, we can also find the numerically based results, where the heat transfer is predicted with the use of sophisticated flow-field modelling techniques, as in Behnia et al. [8] or Merci and Dick [9]. All the above studies aim to find the heat transfer characteristics in the jet impingement systems, but this task has been approached only approximately till now.

The two approaches, experiment and numerical simulation, are coupled by Tomba and Cavalieri [10] in their thermal shock behaviour considerations on alumina disks, where they use a simplified model for the heat transfer radial distribution. However, among the first to study the functionally graded materials in this context seem to be Elperin and Rudin [11], Kim and Noda [12], and Sadowski and Neubrand [13,14], where the specimen made of Al_2O_3/Al is tested.

The current work focuses mainly on finding a simple and efficient method of modelling the heat transfer coefficient and conduction phenomena that occur during the shock test of the FGM specimens made of Al_2O_3/ZrO_2. The problem is treated in two stages. First the inverse heat transfer problem is solved for the monolithic specimen and the heat transfer coefficient is thus obtained. The temperature field in FGM plates is found in the second step based on previous surface heat transfer data and by using the finite difference numerical methodology for the solution of the unsteady heat conduction equation.

2. Experimental procedure

2.1. Specimen preparation

Two types of materials were prepared: Al_2O_3 and FGM Al_2O_3/ZrO_2 made of pure alumina powder from Skawina (Poland) and 3 mol% yttria stabilised tetragonal ZrO_2 powder from Zhongshun Sci & Tech. (China). Cylindrical plates (diameter $d = 30$ mm and thickness $w = 2.5$ mm) were finally obtained. FGM samples were made by sequentially stacking 5 layers (each 0.5 mm thick) containing 0, 5, 10, 15 and 20 wt%ZrO_2 (Fig. 1). Subsequently the obtained plates were uniaxially pressed under pressure of 10 MPa,

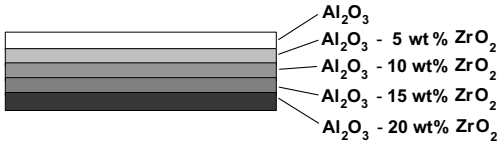

Fig. 1. FGM samples.

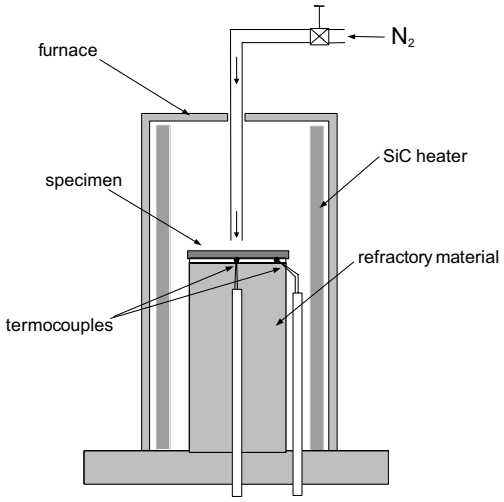

Fig. 2. Scheme of the thermal shock stand.

isostatically pressed at 120 MPa, sintered at 1973 K for 1.5 h in air and were polished at one (Al_2O_3) side.

2.2. Thermal shock test

The plates were subjected to non-symmetric thermal shock in the following way (Fig. 2). The samples were heated in a furnace to predetermined temperatures (1023, 1073, 1123 K) and next subjected to sudden temperature change using a high-velocity nitrogen jet (about 17 l/min) at room temperature. The gas was channelled onto the disk centre for about 20 s, using a metal tube (inner diameter $D = 4.5$ mm) placed perpendicularly and 3 mm above the test surface (polished). During the gas impinging the variation of temperature was recorded on the lower sample surface at the central point and a peripheral one (located 14.5 mm from the centre) with aid of Pt–Rh/Pt thermocouples.

3. Theoretical modelling of the heat transfer during cooling process of specimens

3.1. Solution of the non-stationary heat conduction equation for layered FGM materials

The theoretical model of the heat conduction problem for the cylindrical specimens considered in this paper is presented in Fig. 3. The governing equation, initial and boundary conditions for the geometry that is being discussed, according to [15], are given by

$$\rho c \frac{\partial T}{\partial t} = k_r \left(\frac{1}{r} \frac{\partial T}{\partial r} + \frac{\partial^2 T}{\partial r^2} \right) + k_z \frac{\partial^2 T}{\partial z^2} + \frac{\partial k_z}{\partial T} \left(\frac{\partial T}{\partial z} \right)^2 \quad \text{for } \{r, z\} \in \Omega \tag{1}$$

$$T(r, z, t = 0) = T_0 \tag{2}$$

$$\frac{\partial T}{\partial z} = 0 \quad \text{for } \{r, z\} \in \Gamma_1 \tag{3}$$

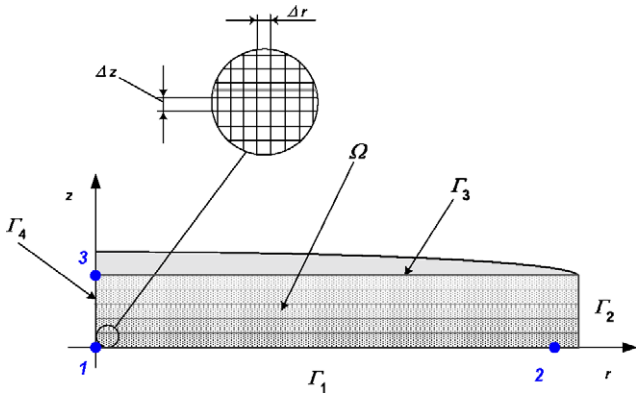

Fig. 3. Computational model.

$$\frac{\partial T}{\partial r} = 0 \quad \text{for } \{r,z\} \in \Gamma_2 \tag{4}$$

$$-k_z \frac{\partial T}{\partial z} - h_3(T - T_3) = 0 \quad \text{for } \{r,z\} \in \Gamma_3 \tag{5}$$

$$\frac{\partial T}{\partial r} = 0 \quad \text{for } \{r,z\} \in \Gamma_4 \tag{6}$$

where the computational domain Ω with its boundary $\Gamma_1 \cup \Gamma_2 \cup \Gamma_3 \cup \Gamma_4$ is defined in Fig. 3. $k_r(r,z,t)$ and $k_z(r,z,t)$ are heat conductions in r and z directions respectively. h_3 and T_3 are the heat transfer coefficient and the fluid temperature over the surface Γ_3. Moreover it is assumed that at the border of different layers the additional conditions of continuity of the: temperature and heat conduction fields are satisfied.

The temperature $T = T(r,z,t)$ is assumed to be independent of the angular coordinate in the above equations (axial symmetry of the problem). The circular cooling jet is directed axially onto the disk, which has uniform material properties in radial/angular direction.

The differential equation is solved by the explicit FTCS finite difference method (e.g. [16,17]), which is stable for Fourier numbers less or equal to the value $\mathrm{Fo}_{\max} = 1/4$. In this work we actually use time steps reduced by approximately 1/3, i.e. $\Delta t = 0.3\ \mathrm{Fo}_{\max}\Delta x^2/\kappa$, where $\Delta x^2 = 1/(1/\Delta r^2 + 1/\Delta z^2)$, and Δr and Δz are computational grid spacings in r- and z-directions, respectively. This enables us to increase the accuracy of the computations and to assure the solution to be smooth enough.

3.2. Thermal properties of monolithic and FGM material

For the purpose of heat transfer modelling, the thermal properties of the specimens were evaluated as follows. The data for the monolithic Al_2O_3 material are based on [10,18] with the heat conduction coefficient being approximated by using the linear function defined in Table 1. In case of zirconia, due to very weak temperature dependency of its thermal conductivity, a mean value $k_r^{ZrO_2} = k_z^{ZrO_2} = 2.93$ W/mK has been assumed, according to the data published in [19]. The heat capacity for ZrO_2 has been derived from the formula:

Table 1
Heat conduction for alumina $k(T) = aT + b$, based on [10]

Temperature range in K	a	b
373–573	−0.06530	53.35700
573–773	−0.02825	32.12700
773–973	−0.01410	21.18900
973–1173	−0.00600	13.30800
1173–1273	−0.00270	9.43700
>1273	0.00000	6.00000

$$c_p^{ZrO_2} = 18.78 + 3.67 \cdot 10^{-3} T - 1310.2(T + 273.15)^{-1} \tag{7}$$

The densities have been estimated at 1023/1073/1123 K temperatures as $\rho^{Al_2O_3} = 3923/3918/3912$ kg/m^3 in case of Al_2O_3 and $\rho^{ZrO_2} = 6060/6057/6054$ kg/m^3 in case of ZrO_2, respectively.

The properties of the FGM material have been evaluated as the weighted averages of the above data, using the zirconia volumetric fractions β as weights, i.e. we use the following formula:

$$k_r^{Al_2O_3/ZrO_2} = k_r^{ZrO_2}\beta + k_r^{Al_2O_3}(1 - \beta) \tag{8}$$

for the heat conductance $k_r^{Al_2O_3/ZrO_2}$ in r-direction. In the same way we define the other material properties. Simplifying the present analysis we neglect the difference between $k_r^{Al_2O_3/ZrO_2}$ and $k_z^{Al_2O_3/ZrO_2}$, which is motivated by small variations of zirconia content between the consecutive material layers (by 5% of weight fraction).

3.3. Proposed model for heat transfer coefficient in monolithic and layered FGM material

The literature reports a number of results that discuss the circular jet impingement heat transfer in case of monolithic disks. The literature data, which have been obtained for the systems similar to the considered here ([3,8]), are presented in Fig. 4. It can be seen that the stagnation-point heat transfer, in case of $H/D = 1$, where H denotes the jet-specimen distance and D is the diameter of the jet, depends approximately in a linear manner on the Reynolds number. The radial distribution of the Nusselt number shows that

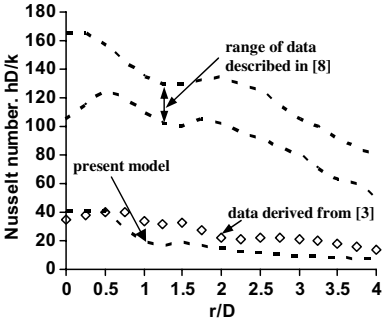

Fig. 4. Radial variations of Nusselt number compared with previous data.

the stagnation-point value is the highest one and that Nu takes local minima with the most significant one in the region $1 < r/D < 1.5$. The numerical predictions and experimental data suggest that the stagnation-point Nusselt number can be estimated in proportion to Re^n, where n takes values from 0.5 to 0.68 (the authors of [8] suggest the exponent 0.62). The radial distribution of heat transfer in the efficient model [10] is defined by means of the piecewise linear and hyperbolic functions. However, the main drawback of their approach is that the resultant function is discontinuous. This drawback is eliminated in the currently suggested model, where an additional curve shape parameter is introduced, resulting in the following function:

$$h(r) = \begin{cases} h_0 & r \leqslant r_0 \\ h_0 \frac{r_0}{r} & r_0 < r \leqslant r_C \\ \frac{r_0}{r_C}\left[\left(h'_0 \frac{r_C}{r'_C} - h_0\right)\frac{r - r_C}{r'_C - r_C} + h_0\right] & \text{if } r_C < r \leqslant r'_C \\ h'_0 \frac{r_0}{r} & r > r'_C \end{cases} \quad (9)$$

where $r_0 < r_C < 4r_0$, $r'_C = r_C + (r_C - r_0)a_C$. Here a_C plays role of the additional curve shape parameter. An example of the above defined curve in terms of the Nusselt number, for $h_0 = 280\ \mathrm{W/m^2\,K}$, $h'_0 = 400\ \mathrm{W/m^2\,K}$, $r_0 = 2.25$ mm, $r_C = 5.7$ mm, and $a_C = 0.3$, is drawn in Fig. 4 with the dashed line.

4. Results and discussion

4.1. Experimental temperature profiles

The experimental temperature profiles are compared with the computation results for two points: 1 and 2 located at the bottom surface, Fig. 3. Point 1 is placed at the symmetry axis, whereas point 2 is peripheral – very close to boundary Γ_2. The curves (Fig. 5) obtained for pure alumina are depicted in part (a) while the simulation results for the composite are shown in part (b). From these figures we can infer that the results for the FGM plates are more accurate if the temperature rises. The error measured in

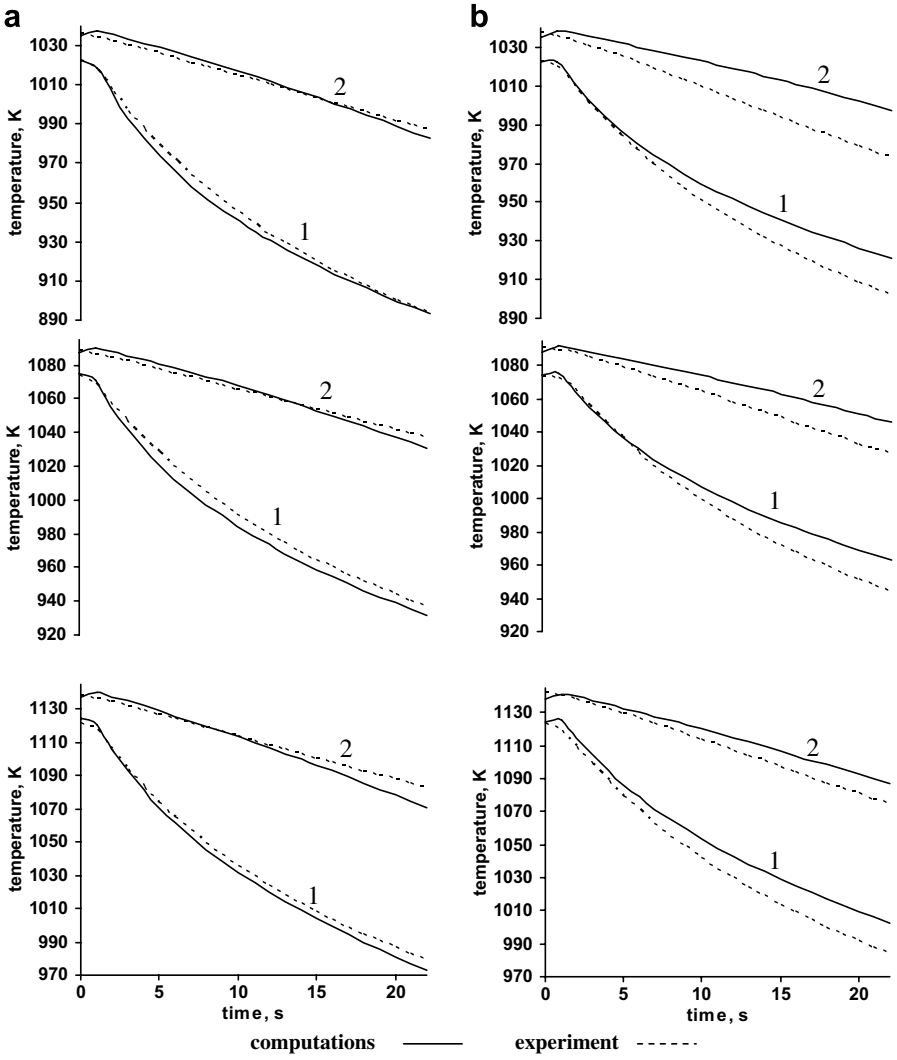

Fig. 5. Comparison of experimental and computed temperature profiles at the bottom central (1) and edge (2) points for the alumina (a) and FGM (b) specimens for various initial conditions.

terms of the experimental and computed temperature difference, related to the maximum temperature drop is bounded between 7 and about 15%, the lowest in case of the initial temperature 1123 K.

4.2. Spatial distributions of temperature

The spatial distributions of calculated temperature are shown in Fig. 6a and b. Part (a) depicts the pure alumina results while part (b) shows the FGM composite temperatures. A small difference between (a) and (b) graphs can be seen in the upper left corner of each one, which represents the adiabatic surface central point. From the observation it is clear that the heat is conducted more slowly in case of the FGM plate. This can be also seen when the final temperature levels are compared.

More exact insight into the heat conduction behaviour of the composite material can be obtained from Fig. 7, where the temperatures at the two points: 1 and 3 situated at the symmetry axis (Fig. 3) are depicted. We can see in this graph that the temperature differences across the specimen thickness in case of monolithic samples are about 6° greater than in the case of the composite material and do not vary substantially with the initial temperatures.

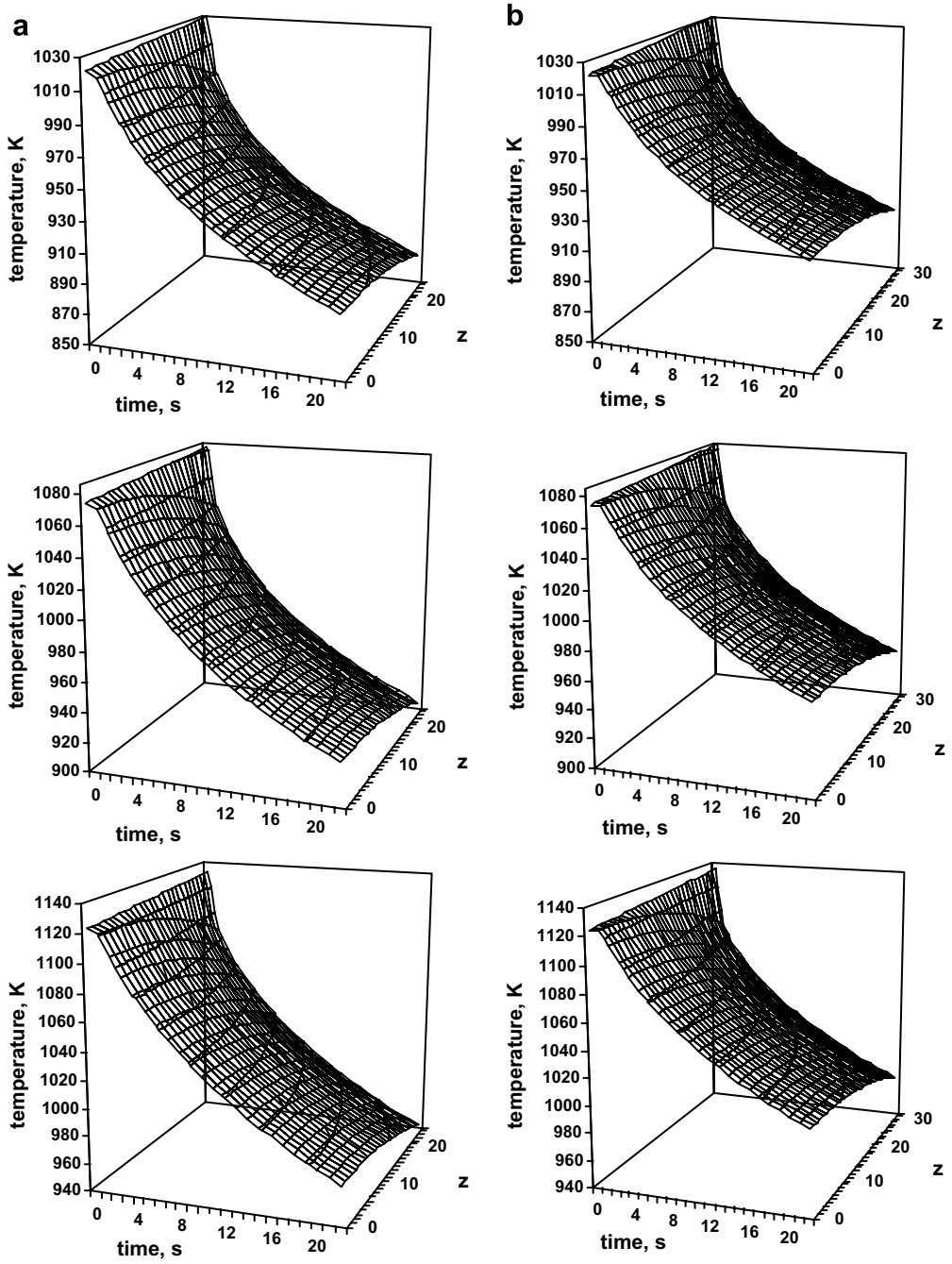

Fig. 6. Axial temperature distributions for the alumina (a) and FGM (b) specimens for various initial conditions.

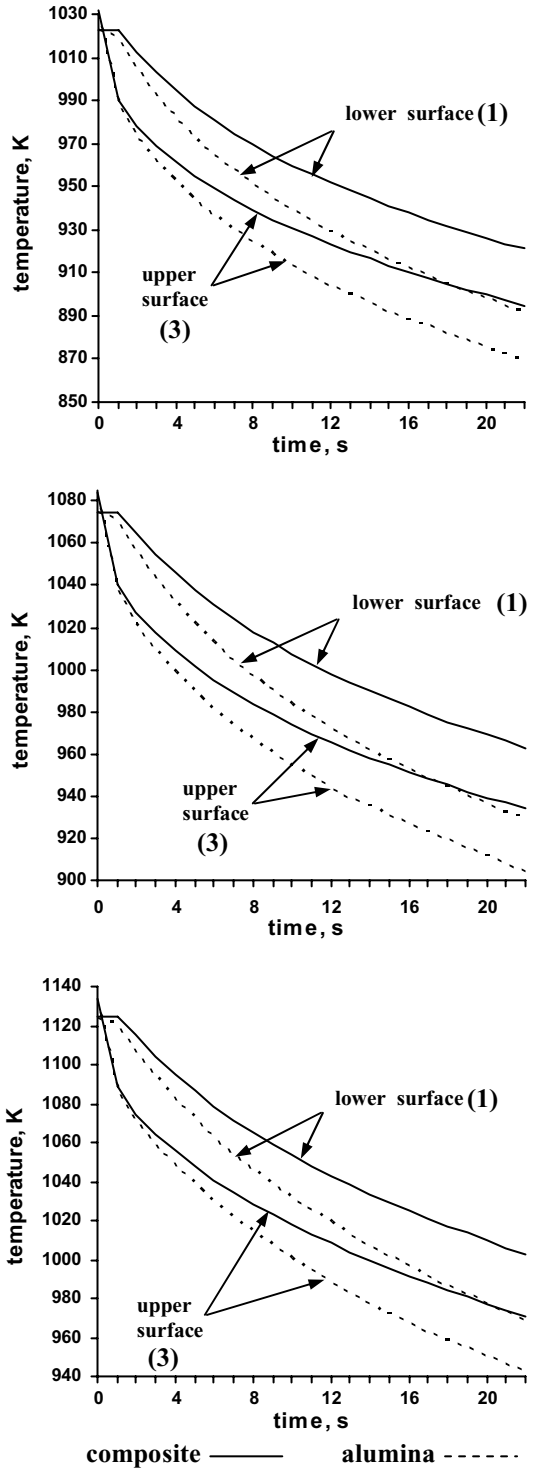

Fig. 7. Comparison of lower- (point 2) and upper-surface (point 3) temperatures for the alumina and FGM specimens for various initial conditions.

5. Final remarks

The paper reports on investigations on the influence of the FGM thermal properties on the temperature distribution inside of the composite material. The study is realised by using a thermal shock test. The heat transfer coefficient is estimated by a simple algebraic model, which is verified in a shock test of a monolithic alumina plate. The predictions of the temperature field in the alumina/zirconium FGM plate can be assessed as qualitatively good in comparison with the experimental data. The quantitative discrepancy that still exists between the measurements and computation results, although not substantial, reveals a need for further enrichment of the computational model.

Acknowledgement

The authors are supported by Polish Ministry of Science and Higher Education – Grant No. 3 T8D 00629.

References

[1] J. Rohde, S. Schmauder, G. Bao, Mesoscopic modelling of gradient zones in hardmetals, Comput. Mater. Sci. 7 (1996) 63–67.
[2] S. Hönle, S. Schmauder, Micromechanical simulation of crack growth in WC/Co using embedded unit cells, Comput. Mater. Sci. 13 (1998) 56–60.
[3] K. Jambunathan, E. Lai, A. Moss, B.L. Button, A review of heat transfer data for single circular jet impingement, Int. J. Heat Fluid Flow 13 (1992) 106–115.
[4] F. Peper, W. Leiner, M. Flebig, Impinging radial and inline jets: a comparison with regard to heat transfer, wall pressure distribution and pressure loss, Exp. Therm. Fluid Sci. 14 (1997) 194–204.
[5] X. Yan, N. Saniei, Heat transfer from an obliquely impinging circular air jet to a flat plate, Int. J. Heat Fluid Flow 18 (1997) 591–599.
[6] E.A. Siba, M. Ganesa-Pillai, K.H. Harris, A. Haji-Sheikh, Heat transfer in a high turbulence air jet impinging over a flat circular disk, ASME J. Heat Transfer 125 (2003) 257–265.
[7] E. Baydar, Y. Ozmen, An experimental investigation on flow structures of confined and unconfined impinging air jets, Heat Mass Transfer 42 (2006) 338–346.
[8] M. Behnia, S. Parneix, Y. Shabany, P.A. Durbin, Numerical study of turbulent heat transfer in confined and unconfined impinging jets, Int. J. Heat Fluid Flow 20 (1999) 1–9.
[9] B. Merci, E. Dick, Heat transfer predictions with a cubic k–ε model for axisymmetric turbulent jets impinging onto a flat plate, Int. J. Heat Mass Transfer 46 (2003) 469–480.
[10] A.G.M. Tomba, A.L. Cavalieri, Evaluation of the heat transfer coefficient in thermal shock of alumina disks, Mater. Sci. Eng. A 267 (2000) 76–82.
[11] T. Elperin, G. Rudin, Thermal reliability testing of functionally gradient materials using thermal shock method, Heat Mass Transfer 36 (2000) 231–236.
[12] K.-S. Kim, N. Noda, A Green's function approach to the deflection of a FGM plate under transient thermal loading, Arch. Appl. Mech. 72 (2002) 127–137.
[13] T. Sadowski, A. Neubrand, Thermal shock crack propagation in functionally graded strip, in: A.M. Brandt, V. Li, I.H. Marshal (Eds.), Brittle Matrix Composites 7, Zturek RSI and Woodhead Publ., Warsaw–Cambridge, 2003, pp. 81–90.
[14] T. Sadowski, A. Neubrand, Estimation of the crack length after thermal shock, Int. J. Fracture 127 (2004) 135–140.
[15] H.S. Carslaw, J.C. Jaeger, Conduction of Heat in Solids, Oxford Clarendon Press, 1959, pp. 39–43.
[16] S. Wiśniewski, Heat load of turbine engines, WKiŁ Warsaw 1974, pp. 207–252 (in Polish).

[17] Y. Jaluria, K.E. Torrance, in: W.J. Minkowycz, E.M. Sparrow (Eds.), Computational heat transfer, Comp. Methods in Mechanics and Thermal Sciences, Hemisphere Publ. Corp., 1986, pp. 79–143.

[18] R.G. Munro, Evaluated material properties for a sintered α-alumina, J. Am. Ceram. Soc. 80 (1997) 1919–1928.

[19] R. Stevens, Zirconia and Zirconia Ceramics, Magnesium Electron Ltd., July, 1986.